Bull. Mater. Sci., Vol. 32, No. 6, December 2009, pp. 603–606. © Indian Academy of Sciences.

Heat capacity measurements on $Yb_xGd_{2-x}Zr_2O_7$ ($x = 0, 1, 2$) ceramics by differential scanning calorimetry

ZHAN-GUO LIU, JIA-HU OUYANG* and YU ZHOU

Institute for Advanced Ceramics, Department of Materials Science, Harbin Institute of Technology, Harbin 150001, P R China

MS received 23 July 2009

Abstract. **$Yb_xGd_{2-x}Zr_2O_7$ ($x = 0, 1, 2$) ceramics were pressureless-sintered using ceramic powders acquired by chemical-coprecipitation and calcination methods. Heat capacities of $Yb_xGd_{2-x}Zr_2O_7$ were measured with a heat flux-type differential scanning calorimetry in the temperature range of 298–1200 K. At 298 K, the heat capacities of $Gd_2Zr_2O_7$, $YbGdZr_2O_7$ and $Yb_2Zr_2O_7$ were 214, 221 and 230 $J \cdot K^{-1}$ mol^{-1}, respectively.**

Keywords. **$Yb_xGd_{2-x}Zr_2O_7$; heat capacity; differential scanning calorimetry; enthalpy.**

1. Introduction

The rare-earth zirconates with the general formula, $Ln_2Zr_2O_7$ (Ln = lanthanide), have high melting points, relatively high thermal expansion coefficients, low thermal conductivities, high stability and ability to accommodate defects. These properties make rare-earth zirconates suitable for a variety of applications such as solid electrolytes, catalysts, nuclear waste forms, and especially thermal barrier coating materials (Lutique *et al* 2003; Cao *et al* 2004; Liu *et al* 2008; Mandal *et al* 2008; Tong *et al* 2008). These compounds exhibit a pyrochlore-type structure or a defect fluorite-type structure, which is mainly governed by the ionic size difference between Ln and Zr sites (Subramanian *et al* 1983). Thermodynamic properties such as heat capacity and enthalpy of these compounds are necessary to understand the behaviour of materials in practice applications. The heat capacities of $Gd_2Zr_2O_7$ were measured by adiabatic calorimetry and the hybrid adiabatic relaxation method in the temperature range of 0·3–400 K (Lutique *et al* 2004). However, there are no measured heat capacity data for $Yb_2Zr_2O_7$ and its solid solutions. In the present paper, heat capacity measurements on $Yb_xGd_{2-x}Zr_2O_7$ ($x = 0, 1, 2$) were carried out by differential scanning calorimetry in the temperature range 298–1200 K.

2. Experimental

2.1 *Sample preparation*

Zirconium oxychloride (Zibo Huantuo Chemical Co. Ltd., China; Analytical), gadolinium oxide and ytterbium oxide powders (Rare-Chem Hi-Tech Co., Ltd., Huizhou, China; purity ≥ 99·99%) were selected as the reactants. Ceramic powders of $Yb_xGd_{2-x}Zr_2O_7$ ($x = 0, 1, 2$) were synthesized by chemical-coprecipitation and calcination methods. Gadolinium oxide and ytterbium oxide powders were heated in air at 1173 K for 2 h to remove any absorbed moisture. For each composition, rare-earth oxide powders were weighed, and dissolved in diluent nitric acid, while zirconium oxychloride was dissolved in distilled water. These solutions were mixed, stirred, filtered and slowly added into a dilute ammonium hydrate solution to obtain gel-like precipitates. These gels were washed with distilled water until pH = 7 and then washed several times in analytically pure alcohol. The obtained precipitates were dried, ground, calcined at 1073 K in air for 5 h and compacted by cold isostatic pressing at 280 MPa for 5 min. Finally, the compacts were pressureless-sintered at 1873 K for 10 h in air. The phase structures of sintered specimens were identified by X-ray diffractometry (Model Rigaku D/Max 2200VPC, Japan) with Cu$K\alpha$ radiation at a scan rate of 4°/min.

2.2 *Heat capacity measurements*

Heat capacity measurements were performed using a heat flux type thermal analyser (Model Netzsch STA 449C Jupiter®, Germany) equipped with a sample holder for differential scanning calorimetry and a Rh furnace in this study. Temperature calibration was carried out by determining the phase transition temperature of rubidium nitrate, potassium perchlorate, silver sulfate, potassium chromate, barium carbonate and strontium carbonate supplied by the National Institute of Standards and Technology, USA (NIST). Heat calibration was carried out by

*Author for correspondence (ouyangjh@hit.edu.cn)

measuring the enthalpies of phase transition of above-mentioned reference materials. Heat rate calibration was performed prior to each heat capacity measurement with a disc of sapphire supplied by Netzsch-Gerätebau GmbH, Germany, using the heat capacity data of sapphire from NIST, USA.

Heat capacity measurements were carried out in the temperature range of 298–1200 K. Disc-shaped samples with dimensions of about 5 mm in diameter and about 0·5 mm in thickness were machined from sintered ceramics. To eliminate any adsorbed moisture on the samples, the samples were heated at 473 K overnight before starting the experiment. The mass of samples were weighed accurately and hermetically sealed in platinum crucible. The flow rate of the purge gas (high pure, N_2 + 20 Vol.% O_2) was 30 mL/min. A three-segment temperature program was used. The first segment was isothermal at 298 K for 10 min; the second segment was from 298 to 1200 K at a heating rate of 20 K min^{-1} and the final segment was holding at 1200 K for 10 min.

Heat capacities of all samples were determined by the classical three-step method in the continuous heating mode (Hohne *et al* 2003). First, a blank run with empty platinum crucibles on both sample and reference sides; second, a sapphire run with empty platinum crucible on the reference side and the platinum crucible with sapphire on the sample side; finally, the sample run with empty platinum crucible on the reference side and the sample on the sample side. The values of heat capacity were calculated by the following equation (Patil *et al* 2007):

$$C_{\mathrm{p,m}}(T)_{\mathrm{sample}} = \left(\frac{HF_{\mathrm{sample}} - HF_{\mathrm{blank}}}{HF_{\mathrm{ref}} - HF_{\mathrm{blank}}}\right) \times \left(\frac{M_{\mathrm{ref}}}{M_{\mathrm{sample}}}\right) C_{\mathrm{p,m}}(T)_{\mathrm{ref}}, \quad (1)$$

where HF_{blank}, HF_{ref} and HF_{sample} represent heat flow during first, second and third runs, respectively; $C_{\mathrm{p,m}}(T)_{\mathrm{sample}}$ and $C_{\mathrm{p,m}}(T)_{\mathrm{ref}}$ represent the heat capacities of the sample and the reference material (sapphire), respectively; and M_{ref} and M_{sample} represent the masses of the reference and the sample, respectively. The experimental uncertainty was estimated at ± 2%.

3. Results and discussion

Figure 1 reveals X-ray diffraction patterns of $Yb_xGd_{2-x}Zr_2O_7$ (x = 0, 1, 2) samples. It can be seen that all $Yb_xGd_{2-x}Zr_2O_7$ ceramics are with a single defect fluorite-type phase structure. The XRD patterns of $Yb_xGd_{2-x}Zr_2O_7$ (x = 0, 2) ceramics agree well with the standard XRD data of $Gd_2Zr_2O_7$ (JCPDS Card No. 80–0471) and $Yb_2Zr_2O_7$ (JCPDS Card No. 78–1300), respectively. The lattice parameters of $Gd_2Zr_2O_7$, $YbGdZr_2O_7$ and $Yb_2Zr_2O_7$ calculated from XRD results are 5·263, 5·217 and 5·167 Å, respectively.

Heat capacity data of $Yb_xGd_{2-x}Zr_2O_7$ ceramics as given in tables 1–3 are the mean values of three measurements, respectively. The error derived from the mean standard deviation for three measurements of each sample is less than 2%. The measured heat capacity $C_{\mathrm{p,m}}$ in the unit of $J{\cdot}K^{-1}{\cdot}mol^{-1}$ for $Yb_xGd_{2-x}Zr_2O_7$ ceramics were fitted using

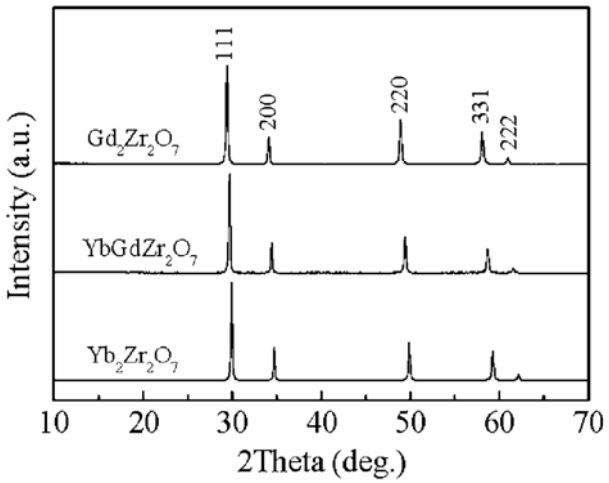

Figure 1. XRD patterns of $Yb_xGd_{2-x}Zr_2O_7$ (x = 0, 1, 2) ceramics.

Table 1. Thermodynamic functions of $Gd_2Zr_2O_7$ at selected temperature.

	$C_{\mathrm{p,m}}$ (J K^{-1} mol^{-1})		
T (K)	Measured	Fit	$H_T^0 - H_{298}^0$ (J mol^{-1})
298	214	213	0
300	215	214	395
450	246	245	32244
600	258	259	65959
750	268	267	100060
900	275	274	134054
1050	277	279	167729
1200	285	284	200978

Table 2. Thermodynamic functions of $YbGdZr_2O_7$ at selected temperature.

	$C_{\mathrm{p,m}}$ (J K^{-1} mol^{-1})		
T (K)	Measured	Fit	$H_T^0 - H_{298}^0$ (J mol^{-1})
298	221	225	0
300	222	226	422
450	259	256	34106
600	270	268	69534
750	274	276	105320
900	282	282	141004
1050	286	287	176386
1200	295	292	211367

least square method to obtain the following polynomial equations as a function of temperature, respectively.

$$C_{p,m}\,(Gd_2Zr_2O_7) = 255{\cdot}25 + 2{\cdot}372 \times 10^{-2}\,T - 4{\cdot}442392 \times 10^{6}\,T^{-2} \quad (298\ \mathrm{K} \le T \le 1200\ \mathrm{K}), \tag{2}$$

$$C_{p,m}\,(YbGdZr_2O_7) = 264{\cdot}78 + 2{\cdot}513 \times 10^{-2}\,T - 4{\cdot}157336 \times 10^{6}\,T^{-2} \quad (298\ \mathrm{K} \le T \le 1200\ \mathrm{K}), \tag{3}$$

$$C_{p,m}\,(Yb_2Zr_2O_7) = 271{\cdot}89 + 3{\cdot}585 \times 10^{-2}\,T - 4{\cdot}527539 \times 10^{6}\,T^{-2} \quad (298\ \mathrm{K} \le T \le 1200\ \mathrm{K}). \tag{4}$$

The standard errors of the fit eqs (2)–(4) are 1·9, 2·5 and 2·1 $J{\cdot}K^{-1}{\cdot}mol^{-1}$, respectively. The measured heat capacity of $Yb_xGd_{2-x}Zr_2O_7$ ceramics in company with the fit values are shown in figures 2–4, respectively. The heat capacities of $Yb_xGd_{2-x}Zr_2O_7$ ceramics calculated as a function of temperature from the chemical compositions of $Yb_xGd_{2-x}Zr_2O_7$ ceramics with the Neumann–Kopp rule (Swalin 1972) and the heat capacity data of the constituent oxides (Yb_2O_3, Gd_2O_3 and ZrO_2) obtained from the literature (Kubaschewsji *et al* 1993) are also given in figures 2–4, respectively. It can be seen that the present data are in good agreement within ± 2% with those computed using Neumann–Kopp rule using the heat capacity data of their respective component oxides. The heat capacity data of $Gd_2Zr_2O_7$ ceramics reported in the literature (Lutique *et al* 2004) are also shown in figure 2. It can be seen that, the present data are slightly lower than those reported in Lutique *et al*'s (2004) work in the corresponding temperature range, which is probably caused by different measurement methods. From (2)–(4), enthalpy of $Yb_xGd_{2-x}Zr_2O_7$ ceramics were computed and are given in tables 1–3, respectively.

It is clearly seen from tables 1–3 that the heat capacities of $Yb_xGd_{2-x}Zr_2O_7$ ceramics approximately increase in the order of $C_{p,m}$ ($Yb_2Zr_2O_7$) > $C_{p,m}$ ($YbGdZr_2O_7$) > $C_{p,m}$ ($Gd_2Zr_2O_7$) at identical temperature levels. The ionic radius of Gd^{3+} (1·053 Å) is larger than that of Yb^{3+} (0·985 Å) in rare-earth zirconates (Rohrer 2004), hence

Table 3. Thermodynamic functions of $Yb_2Zr_2O_7$ at selected temperature.

	$C_{p,m}$ (J K^{-1} mol^{-1})		
T (K)	Measured	Fit	$H_T^0 - H_{298}^0$ (J mol^{-1})
298	230	232	0
300	230	232	421
450	266	265	34208
600	281	281	69801
750	291	291	105647
900	298	299	141228
1050	304	305	176324
1200	314	312	210822

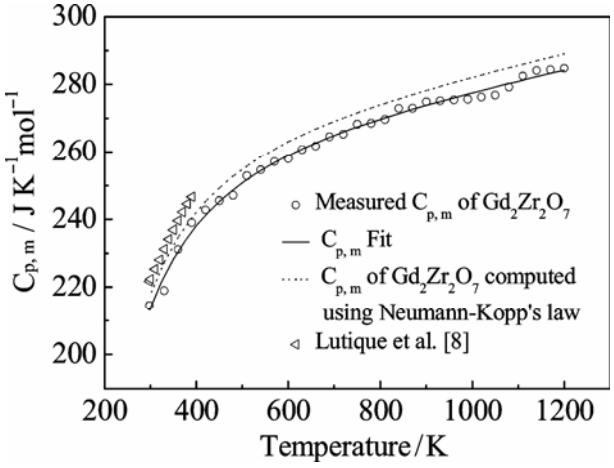

Figure 2. Heat capacity data of $Gd_2Zr_2O_7$.

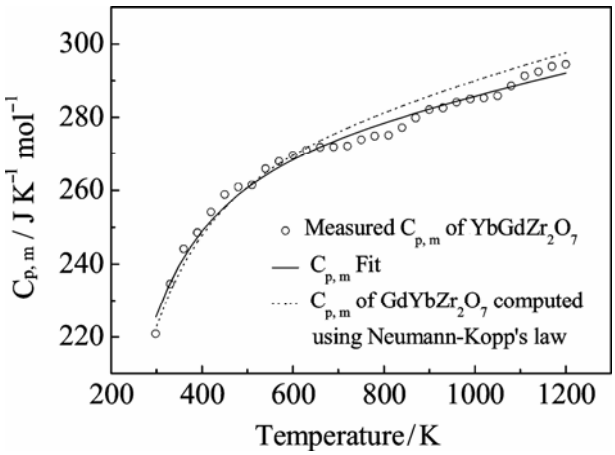

Figure 3. Heat capacity data of $YbGdZr_2O_7$.

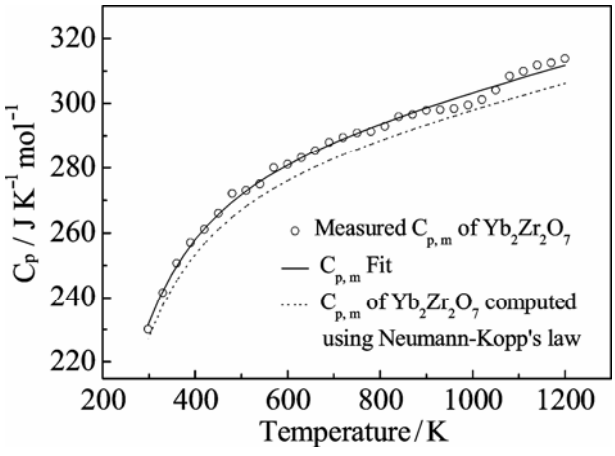

Figure 4. Heat capacity data of $Yb_2Zr_2O_7$.

the Gd–O ionic bond length is larger than the Yb–O ionic bond length. This is consistent with the lattice parameter from above XRD results, which decreases from $x = 0$ ($Gd_2Zr_2O_7$) to $x = 2$ ($Yb_2Zr_2O_7$). The shorter the ionic bond length, the higher will be the bond strength (Gavarri and Chater 1988), and consequently the higher will be the heat capacity, which agrees well with the measured results in this study.

4. Conclusions

$Yb_xGd_{2-x}Zr_2O_7$ ($x = 0$, 1, 2) ceramics were pressureless-sintered using ceramic powders acquired by chemical-coprecipitation and calcination methods at 1873 K for 10 h in air. The $Yb_xGd_{2-x}Zr_2O_7$ exhibits a defect fluorite-type structure. The heat capacities of $Yb_xGd_{2-x}Zr_2O_7$ ceramics approximately increase in the order of $C_{p,m}(Yb_2Zr_2O_7) > C_{p,m}$ ($YbGdZr_2O_7$) > $C_{p,m}(Gd_2Zr_2O_7)$ at identical temperature levels. At 298 K, the heat capacities of $Gd_2Zr_2O_7$, $YbGdZr_2O_7$ and $Yb_2Zr_2O_7$ are 214, 221 and 230 $J{\cdot}K^{-1}{\cdot}mol^{-1}$, respectively.

Acknowledgements

The authors would like to thank the financial support from the Program of Excellent Teams in Harbin Institute of Technology (HIT), the Start-up Program for High-level HIT Faculty Returned from Abroad and the National Natural Science Foundation of China (NSFC-No. 50972030).

References

Cao X Q, Vassen R and Stőever D 2004 *J. Eur. Ceram. Soc.* **24** 1

Gavarri J R and Chater R 1988 *J. Solid State Chem.* **73** 305

Hohne G W H, Hemminger W F and Flammershein H -J 2003 *Differential scanning calorimetry* (Berlin: Springer) 2nd edn

Kubaschewsji O, Alcock C B and Spencer P J 1993 *Materials thermochemistry* (Oxford: Pergamon Press) 6th edn

Liu Z -G, Ouyang J -H and Zhou Y 2008 *J. Mater. Sci.* **43** 3596

Lutique S, Staicu D, Konings R J M, Rondinella V V, Somers J and Wiss T 2003 *J. Nucl. Mater.* **319** 59

Lutique S, Javorskỳ P, Konings R J M, Krupa J -C, van Genderen A C G, van Miltenburg J C and Wastin F 2004 *J. Chem. Thermodyn.* **36** 609

Mandal B P, Deshpande S K and Tyagi A K 2008 *J. Mater. Res.* **23** 911

Patil A, Parida S C, Dash S and Venugopal V 2007 *Thermochim. Acta* **465** 25

Rohrer G S 2004 *Structure and bonding in crystalline materials* (Cambridge: Cambridge University Press)

Subramanian M A, Aravamudan G and Subba Rao G V 1983 *Prog. Solid State Chem.* **15** 55

Swalin R A 1972 *Thermodynamics of solids* (New York: John Wiley & Sons) 2nd edn

Tong Y, Zhu J, Lu L, Wang X and Yang X 2008 *J. Alloys Compd.* **465** 280